Article

Biomimetic Interactions of Proteins with Functionalized Nanoparticles: A Thermodynamic Study

Mrinmoy De, Chang-Cheng You, Sudhanshu Srivastava, and Vincent M. Rotello

J. Am. Chem. Soc., **2007**, 129 (35), 10747-10753• DOI: 10.1021/ja071642q • Publication Date (Web): 02 August 2007

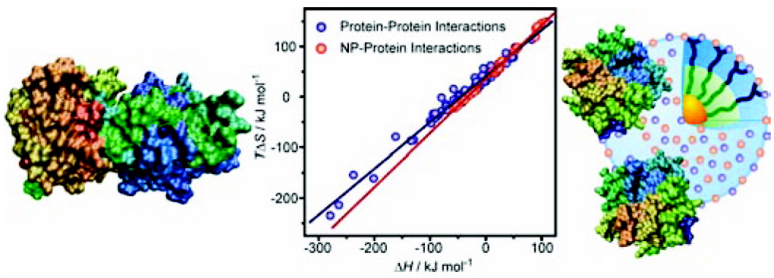

More About This Article

Additional resources and features associated with this article are available within the HTML version:

- Supporting Information
- Links to the 5 articles that cite this article, as of the time of this article download
- Access to high resolution figures
- Links to articles and content related to this article
- Copyright permission to reproduce figures and/or text from this article

View the Full Text HTML

J|A|C|S
ARTICLES
Published on Web 08/02/2007

Biomimetic Interactions of Proteins with Functionalized Nanoparticles: A Thermodynamic Study

Mrinmoy De, Chang-Cheng You, Sudhanshu Srivastava, and Vincent M. Rotello*

Contribution from the Department of Chemistry, University of Massachusetts, 710 North Pleasant Street, Amherst, Massachusetts 01003

Received March 8, 2007; E-mail: rotello@chem.umass.edu

Abstract: Gold nanoparticles (NPs) functionalized with L-amino acid-terminated monolayers provide an effective platform for the recognition of protein surfaces. Isothermal titration calorimetry (ITC) was used to quantify the binding thermodynamics of these functional NPs with α-chymotrypsin (ChT), histone, and cytochrome *c* (CytC). The enthalpy and entropy changes for the complex formation depend upon the nanoparticle structure and the surface characteristics of the proteins, e.g., distributions of charged and hydrophobic residues on the surface. Enthalpy−entropy compensation studies on these NP−protein systems indicate an excellent linear correlation between ΔH and $T\Delta S$ with a slope (α) of 1.07 and an intercept ($T\Delta S_0$) of 35.2 kJ mol^{-1}. This behavior is closer to those of native protein−protein systems ($\alpha = 0.92$ and $T\Delta S_0 = 41.1$ kJ mol^{-1}) than other protein−ligand and synthetic host−guest systems.

Introduction

Biomimetic chemistry provides a valuable tool for the understanding of biological processes as well as a tool for the creation of functional synthetic systems. Enzymes provide an important target for the creation of biomimetic systems, with a vast array of enzyme and metalloenzyme active site model systems having been developed.[1] In contrast to active site models, there have been far fewer efforts to model the *exterior* of proteins, in particular their interactions with other biomacromolecules. Effective mimicking of protein surfaces would provide fundamental insight into issues such as protein−protein and protein−nucleic acid interactions. Additionally, replication of protein surface behavior provides access to useful catalysts,[2] sensors,[3] and therapeutics.[4]

Nanoparticles provide excellent systems for modeling protein surfaces. In particular, they can be readily fabricated with dimensions comparable to biological macromolecules.[5] Moreover, the synthetic control we can exert on the ligands can be used to tune the structure and dynamics of the monolayer surface. For example, peptide-functionalized NPs have been constructed to function as artificial proteins and enzymes,[6] glyconanoparticles have been used as useful models of cell adhesion,[7] and a variety of functionalized particles have been used for recognition in aqueous media.[8,9] Likewise, nanoparticle−protein interactions have found promising applications in modulation of enzymatic activity,[10] biosensing,[11] separation,[12] and production of hybrid materials.[13]

(1) (a) Breslow, R. Ed. *Artificial Enzymes*; Wiley-VCH: Weinheim, 2005. (b) Thomas, C. M.; Ward, T. R. *Chem. Soc. Rev.* **2005**, *34*, 337−346.
(2) (a) Thordarson, P.; Bijsterveld, E. J. A.; Rowan, A. E.; Nolte, R. J. M. *Nature* **2003**, *424*, 915−918. (b) Uyemura, M.; Aida, T. *J. Am. Chem. Soc.* **2002**, *124*, 11392−11403.
(3) (a) Favero, G.; Campanella, L.; Cavallo, S.; D'Annibale, A.; Perrella, M.; Mattei, E.; Ferri, T. *J. Am. Chem. Soc.* **2005**, *127*, 8103−8111. (b) Ye, L.; Haupt, Anal, K. *Bioanal. Chem.* **2004**, *378*, 1887−1897. (c) Song, X. D.; Swanson, B. I. *Anal. Chem.* **1999**, *71*, 2097−2107. (d) Kaifer, A. E. *Acc. Chem. Res.* **1999**, *32*, 62−71. (e) Cornell, B. A.; BraachMaksvytis, V. L. B.; King, L. G.; Osman, P. D. J.; Raguse, B.; Wieczorek, L.; Pace, R. J. *Nature* **1997**, *387*, 580−583.
(4) (a) Yoshida, R. *Curr. Org. Chem.* **2005**, *9*, 1617−1641. (b) Esfand, R.; Tomalia, D. A. *Drug Discovery Today* **2001**, *6*, 427−436. (c) Yamazaki, N.; Kojima, S.; Bovin, N. V.; Andres, S.; Gabius, S.; Gabius, H. J. *Adv. Drug Delivery Rev.* **2000**, *42*, 225−244.
(5) Hostetler, M. J.; Wingate, J. E.; Zhong, C. J.; Harris, J. E.; Vachet, R. W.; Clark, M. R.; Londono, J. D.; Green, S. J.; Stokes, J. J.; Wignall, G. D.; Glish, G. L.; Porter, M. D.; Evans, N. D.; Murray, R. W. *Langmuir* **1998**, *14*, 17−30.
(6) (a) Pengo, P.; Baltzer, L.; Pasquato, L.; Scrimin, P. *Angew. Chem., Int. Ed.* **2007**, *46*, 400−404. (b) Pengo, P.; Polizzi, S.; Pasquato, L.; Scrimin, P. *J. Am. Chem. Soc.* **2005**, *127*, 1616−1617. (c) Levy, R. *Chem. Biol. Chem.* **2006**, *7*, 1141−1145.
(7) (a) de la Fuente, J. M.; Barrientos, A. G.; Rojas, T. C.; Rojo, J.; Canada, J.; Fernandez, A.; Penades, S. *Angew. Chem., Int. Ed.* **2001**, *40*, 2257−2261. (b) de la Fuente, J. M.; Eaton, P.; Barrientos, A. G.; Menendez, M.; Penades, S. *J. Am. Chem. Soc.* **2005**, *127*, 6192−6197. (c) de Souza, A. C.; Halkes, K. M.; Meeldijk, J. D.; Verkleij, A. J.; Vliegenthart, J. F. G.; Kamerling, J. P. *Chem. Biol. Chem.* **2005**, *6*, 828−831. (d) de Souza, A. C.; Kamerling, J. P. *Methods Enzymol.* **2006**, *417*, 221−243.
(8) (a) You, C.-C.; Verma, A.; Rotello, V. M. *Soft Matter* **2006**, *2*, 190−204. (b) Rosi, N. L.; Mirkin, C. A. *Chem. Rev.* **2005**, *105*, 1547−1562. (c) Verma, A.; Rotello, V. M. *Chem. Commun.* **2005**, 303−312. (d) Daniel, M.-C.; Astruc, D. *Chem. Rev.* **2004**, *104*, 293−346. (e) Pasquato, L.; Pengo, P.; Scrimin, P. *J. Mater. Chem.* **2004**, *14*, 3481−3487. (f) Katz, E.; Willner, I. *Angew. Chem., Int. Ed.* **2004**, *43*, 6042−6108. (g) Shenhar, R.; Rotello, V. M. *Acc. Chem. Res.* **2003**, *36*, 549−561. (h) Sastry, M.; Rao, M.; Ganesh, K. N. *Acc. Chem. Res.* **2002**, *35*, 847−855.
(9) (a) Nam, J.-M.; Stoeva, S. I.; Mirkin, C. A. *J. Am. Chem. Soc.* **2004**, *126*, 5932−5933. (b) Verma, A.; Nakade, H.; Simard, J. M.; Rotello, V. M. *J. Am. Chem. Soc.* **2004**, *126*, 10806−10807. (c) Zheng, M.; Huang, X. *J. Am. Chem. Soc.* **2004**, *126*, 12047−12054. (d) Raschke, G.; Kowarik, S.; Franzl, T.; Sönnichsen, C.; Klar, T. A.; Feldmann, J.; Nichtl, A.; Kürzinger, K. *Nano Lett.* **2003**, *3*, 935−938. (e) Wilson, R. *Chem. Commun.* **2003**, 108−109. (f) Wang, G.; Zhang, J.; Murray, R. W. *Anal. Chem.* **2002**, *74*, 4320−4327. (g) Cao, Y. C.; Jin, R.; Mirkin, C. A. *Science* **2002**, *297*, 1536−1540. (h) McIntosh, C. M.; Esposito, E. A.; Boal, A. K.; Simard, J. M.; Martin, C. T.; Rotello, V. M. *J. Am. Chem. Soc.* **2001**, *123*, 7626−7629. (i) Nath, N.; Chilkoti, A. *J. Am. Chem. Soc.* **2001**, *123*, 8197−8202.
(10) (a) You, C.-C.; Agasti, S. S.; De, M.; Knapp, M. J.; Rotello, V. M. *J. Am. Chem. Soc.* **2006**, *128*, 14512−14618. (b) Hong, R.; Emrick, T.; Rotello, V. M. *J. Am. Chem. Soc.* **2004**, *126*, 13572−12573.
(11) Tsai, C.-S.; Yu, T.-B.; Chen, C.-T. *Chem. Commun.* **2005**, 4273−4275.
(12) Xu, C.; Xu, K.; Gu, H.; Zhong, X.; Guo, Z.; Zheng, R.; Zhang, X.; Xu, B. *J. Am. Chem. Soc.* **2004**, *126*, 3392−3393.
(13) Costanzo, P. J.; Patten, T. E.; Seery, T. A. P. *Chem. Mater.* **2004**, *16*, 1775−1785.

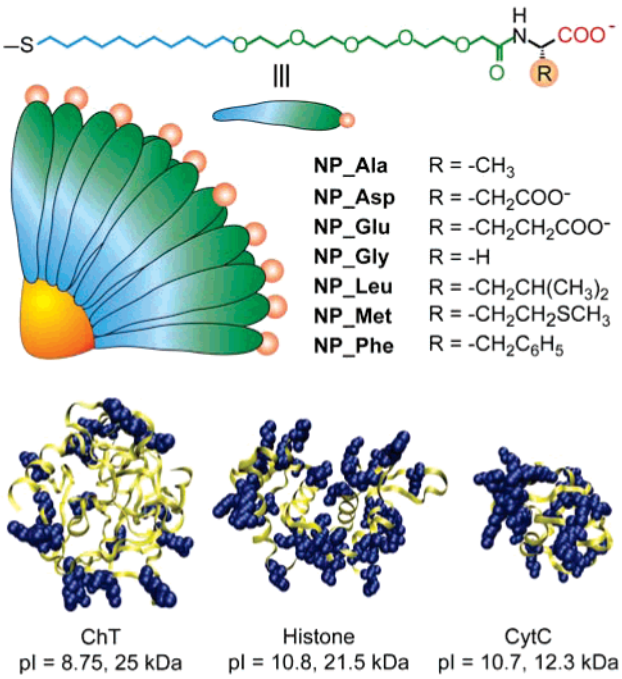

Figure 1. Structural features and relative sizes of amino acid-functionalized gold nanoparticles and proteins. The blue overlapping spheres in the proteins represent the positively charged residues on their surface.

Two distinct approaches have been used to engineer the protein−nanoparticle interface. The first strategy uses the direct introduction of highly specific binding moieties onto the particle surface. For example, biotin-tagged NPs exhibit high affinity interactions with proteins of avidin family.[9c,14] An alternative approach is to utilize the nanoparticle as a multivalent scaffold for the presentation of simple ligands. With this approach the structural attributes of the nanoparticle are brought to bear, including the ability to generate the multiple electrostatic, hydrophobic, and hydrogen-bonding interactions that are found in typical protein−protein interactions.[15,16]

Amino acids present a readily accessed source of the electrostatic, hydrogen bonding, and hydrophobic elements found in proteins. Our previous investigations have demonstrated that amino acid-terminated gold NPs can effectively interact with positively charged proteins, showing tunable inhibition of the enzymatic activity.[17] From binding assays, we observed that complementary electrostatic interactions and hydrophobic interactions between nanoparticles and proteins govern complex formation.

In this report, we investigate the thermodynamics of nanoparticle−protein interactions using isothermal titration calorimetry (ITC). As shown in Figure 1, we choose structurally diverse anionic amino acid-functionalized gold particles as the protein receptors and explored their interactions with three positively charged proteins: α-chymotrypsin (ChT), histone, and cytochrome *c* (CytC). The thermodynamic parameters obtained from ITC studies revealed dramatic differences in the mode of interaction, with the complexation of NPs with ChT enthalpy-driven while the complexation with histone and CytC is entropy-driven. Enthalpy−entropy compensation analysis indicates an excellent linear correlation between these two sets of thermodynamic quantities. Significantly, the compensation coefficients of nanoparticle−protein binding closely resemble that of natural protein−protein interactions, demonstrating the biomimetic nature of these systems.

Results and Discussion

Isothermal Titration Calorimetry. While differential scanning calorimetry (DSC) has been used to characterize NP−protein systems, this technique provides only partial information on binding thermodynamics.[18] ITC has been extensively used to investigate biomacromolecular interactions, directly providing the free energy and enthalpy of association, and the entropy from the former two values.[19]

We fabricated several anionic gold NPs bearing various L-amino acid functionalities to examine their interactions with ChT, histone, and CytC. These proteins have an overall positive charge, albeit with different surface characteristics (refer to Figure 1). ITC experiments were carried out at 30 °C by titrating protein solutions into the sample cell containing nanoparticles. As can be seen from the titration curves (Figure 2), the three NP−protein systems exhibit distinctly different heat change profiles. The complexation of ChT with **NP_Phe** is exothermic, while the complexation of histone with **NP_Ala** or CytC with **NP_Glu** involves endothermic processes. The heat changes can be fitted into isothermal functions to quantify the corresponding thermodynamic parameters of NP−protein interactions. Interestingly, the complexation of NPs with both ChT and histone can be fitted using the mode of single set of identical binding sites. By contrast, the complexation of NPs with CytC can only be assessed using a binding mode of two sets of binding sites. The binding constants (K_S), enthalpy changes (ΔH), and binding stoichiometries (n) were determined from curve-fitting analyses. The Gibbs free energy changes (ΔG) and entropy changes (ΔS) were calculated by using the standard thermodynamic equations $\Delta G = -RT \ln K_S$ and $\Delta G = \Delta H - T\Delta S$. The thermodynamic quantities for the NP−protein interactions are summarized in Table 1.

Nanoparticles afford drastically different binding stoichiometries with the proteins (Table 1) that depend on both the functionality of NPs and the protein type.[20] For example, ChT and histone possess similar molecular sizes, but the latter

(14) (a) Oh, E.; Hong, M.-Y.; Lee, D.; Nam, S.-H.; Yoon, H. C.; Kim, H.-S. *J. Am. Chem. Soc.* **2005**, *127*, 3270−3271. (b) Aslan, K.; Luhrs, C. C.; Perez-Luna, V. H. *J. Phys. Chem. B* **2004**, *108*, 15631−15639. (c) Nagasaki, Y.; Ishii, T.; Sunaga, Y.; Watanabe, Y.; Otsuka, H.; Kataoka, K. *Langmuir* **2004**, *20*, 6396−6400.
(15) (a) Conte, L. L.; Chothia, C.; Janin, J. *J. Mol. Biol.* **1999**, *285*, 2177−2198. (b) Stites, W. E. *Chem. Rev.* **1997**, *97*, 1233−1250. (c) Jones, S.; Thornton, J. M. *Proc. Natl. Acad. Sci. U.S.A.* **1996**, *93*, 13−20.
(16) (a) Bogan, A. A.; Thorn, K. S. *J. Mol. Biol.* **1998**, *280*, 1−9. (b) Lijnzaad, P.; Argos, P. *Proteins* **1997**, *28*, 333−343.
(17) (a) You, C-C.; De, M.; Han, G.; Rotello, V. M. *J. Am. Chem. Soc.* **2005**, *127*, 12873−12881. (b) Bayraktar, H.; You, C.-C.; Rotello, V. M.; Knapp, M. J. *J. Am. Chem. Soc.* **2007**, *129*, 2732−2733.
(18) (a) Larsericsdotter, H.; Oscarsson, S.; Buijs, J. *J. Colloid Interface Sci.* **2004**, *276*, 261−268. (b) Larsericsdotter, H.; Oscarsson, S.; Buijs, J. *J. Colloid Interface Sci.* **2005**, *289*, 26−35.
(19) (a) Jelesarvo, I.; Bosshard, H. I. *J. Mol. Recognit.* **1999**, *12*, 3−18. (b) Wang, R. B.; Schmiedel, H.; Paulke, B. R. *Colloid Polym. Sci.* **2004**, *283*, 91−97. (c) Gourishankar, A.; Shukla, S.; Ganesh, K. N.; Sastry, M. *J. Am. Chem. Soc.* **2004**, *126*, 13186−13187. (d) Joshi, H.; Shirude, P. S.; Bansal, V.; Ganesh, K. N.; Sastry, M. *J. Phys. Chem. B* **2004**, *108*, 11535−11540. (e) Zeng, H. Q.; Yang, X. W.; Flowers, R. A.; Gong, B. *J. Am. Chem. Soc.* **2002**, *124*, 2903−2910.
(20) Based on a model of smaller spheres packing on the surface of a larger sphere, the maximum binding stoichiometries of the nanoparticles ($r \sim 5$ nm) with α-chymotrypsin ($r \sim 2.5$ nm), cytochrome *c* ($r \sim 1.8$ nm), and histone ($r \sim 2.1$ nm) are evaluated as 28, 48, and 37, respectively. For the guideline regarding the calculation, see: Qi, K.; Ma, Q.-G.; Remsen, E. E.; Clark, C. G.; Wooley, K. L. *J. Am. Chem. Soc.* **2004**, *126*, 6599−6607.

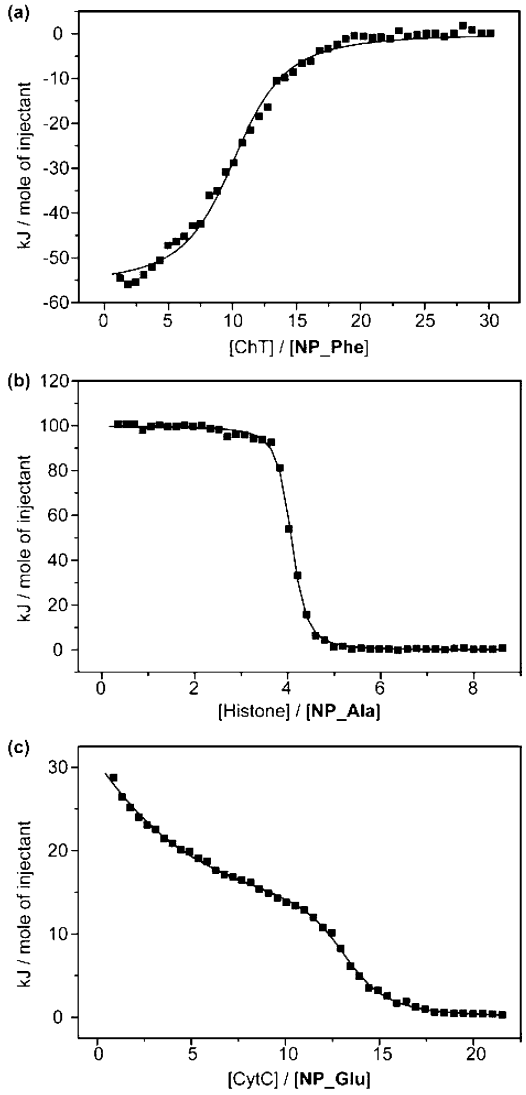

Figure 2. ITC analyses for the complexation of (a) ChT with **NP_Phe**, (b) histone with **NP_Ala**, and (c) CytC with **NP_Glu** in 5 mM sodium phosphate buffer (pH = 7.4). The squares represent the integrated heat changes during complex formation and the lines the curve fit to the binding isothermal functions.

exhibits significantly lower binding ratios to the NPs. On the other hand, the binding capacity of **NP_Glu** with ChT is almost twice that of other NPs, although they have comparable surface area. Structurally, histone has more positively charged residues in comparison with ChT (62 versus 17), while **NP_Glu** possesses double anionic carboxylate functionalities. Taking this information into account, it is reasonable to conclude that the complexation stoichiometries are determined by the ion pairs involved in electrostatic interactions. In other words, if the particle has more electrostatic recognition elements (i.e., carboxylates) it can bind more proteins; likewise if the protein has more cationic residues on the surface it requires more NP partners to form supramolecular complexes.

It is noteworthy that the complexation of NPs with CytC features two distinct binding processes, with markedly differing affinities. For particle−CytC complexation, the first interaction involves a ∼2:1 binding ratio of CytC to NP with binding constants ∼ 10^7 M^{-1}, with the subsequent binding much weaker with binding stoichiometries from 4 to 11. By considering the isotropic surfaces of NPs against ChT and histone, it seems that

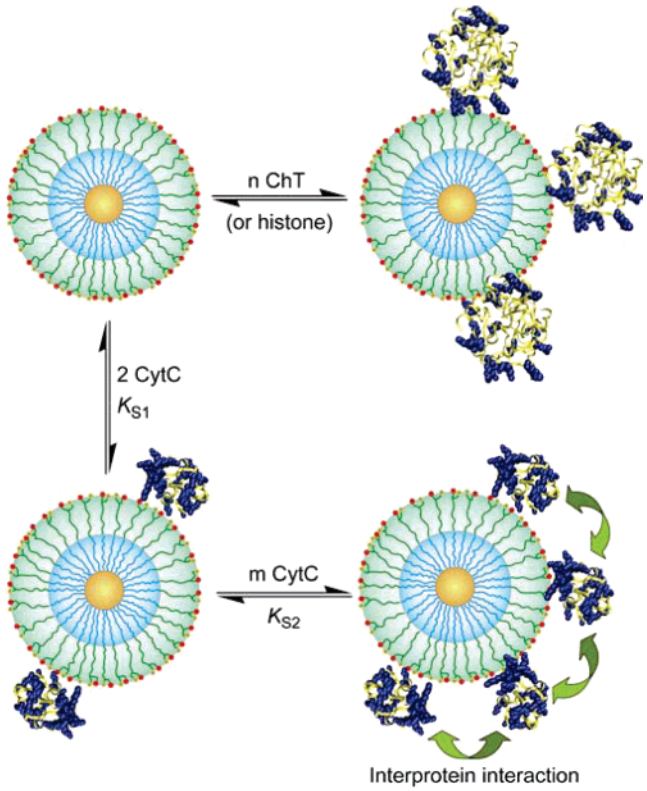

Figure 3. Schematic illustration for the binding modes of CytC with amino acid-functionalized NPs in comparison with that of ChT and histone.

the observed phenomena arise from the unique structural features of CytC. It has been demonstrated that with an increase in protein concentration, CytC molecules undergo reorientation on the surface of citrate-coated silver NPs to facilitate interprotein interactions.[23] In this context, the orientation change and interprotein attraction/repulsion may account for the binding modes of CytC to NPs. The two CytC molecules initially bound may orient themselves opposite from each other to afford the highest binding affinity. Further bound CytC would generate unfavorable interprotein interactions due to electrostatic repulsion (Figure 3). A second explanation can be provided by the monolayer model recently proposed by Stellacci et al. In this model, the ligands on two hemispheres of the particle feature opposing tilt angles, resulting in the appearance of two poles with distinct ligand arrangement.[24] Thus, an alternative explanation for the binding stoichiometries of NP to CytC could be

(21) The binding constants for NP−ChT interactions are around ∼10-fold lower than those obtained from enzyme activity assays (ref 17a), presumably because of the fact that in the latter case (i) the final solution contained 8% (v/v) of ethanol-DMSO (90:10) in the 5 mM phosphate buffer, (ii) 2 mM of *N*-succinyl-L-phenylalanine *p*-nitroanilide (SPNA) was presented as an enzyme substrate would be expected to interfere in the protein−NP interactions, and (iii) the protein concentrations for the ITC are ∼10-fold higher than those used in the activity assay, which would be expected to raise the ionic strength of the solution because of the polyelectrolyte nature of the protein.

(22) NP concentrations were calculated on the basis of their average molecular weights (see Experimental Section and Supporting Information). Thus, the binding stoichiometrics between NPs and ChT differ slightly from previously reported stoichiometrics (ref 17a), where the NP concentrations were calibrated according to the UV absorbance of the gold core (see: Link, S.; Wang, Z.-L.; El-Sayed, M. A. *J. Phys. Chem. B* **1999**, *103*, 3529−3533).

(23) Macdonald, I. D. G.; Smith, W. E. *Langmuir* **1996**, *12*, 706−713.

(24) (a) DeVries, A. G.; Brunnbauer, M.; Hu, Y.; Jackson, A. M.; Long, B.; Neltner, B. T.; Uzun, O.; Wunsch, B. H.; Stellacci, F. *Science* **2007**, *315*, 358−361. (b) Jackson, A. M.; Hu, Y.; Silva, P. J.; Stellacci, F. *J. Am. Chem. Soc.* **2006**, *128*, 11135−11149.

Table 1. Complex Stability Constants (K_S), Gibbs Free Energy Changes (ΔG), Enthalpy Changes (ΔH), Entropy Changes ($T\Delta S$), and Binding Stoichiometries (n) for the Complexation of ChT, Histone, and CytC with Various Amino Acid-Functionalized Gold NPs (5 mM Sodium Phosphate, pH 7.4) at 30 °C

		first binding event					second binding event				
protein	NPs	K_{S1}/M^{-1}	$-\Delta G$/kJ mol^{-1}	ΔH/kJ mol^{-1}	$T\Delta S$/kJ mol^{-1}	n	K_{S2}/M^{-1}	$-\Delta G$/kJ mol^{-1}	ΔH/kJ mol^{-1}	$T\Delta S$/kJ mol^{-1}	n
ChT[21,22]	**NP_Glu**	5.2×10^5	33.2	−52.1	−18.9	23.6					
	NP_Gly	3.6×10^5	32.2	−38.7	−6.4	7.3					
	NP_Leu	7.8×10^5	34.2	−38.7	−13.9	9.7					
	NP_Phe	8.6×10^5	34.4	−56.2	−21.7	10.2					
histone	**NP_Ala**	6.8×10^7	45.6	90.1	135.7	3.5					
	NP_Gly	6.2×10^7	45.1	100.7	145.8	4.0					
	NP_Met	1.2×10^8	46.9	92.6	139.5	3.5					
CytC	**NP_Ala**	1.0×10^7	40.7	51.6	92.3	1.8	4.5×10^5	32.8	15.7	48.6	5.5
	NP_Glu	1.1×10^7	41.0	56.5	97.5	2.0	3.1×10^6	37.6	12.5	50.1	11.1
	NP_Gly	1.0×10^7	40.7	107.7	148.3	2.2	2.0×10^5	30.6	88.7	119.3	4.2
	NP_Met	1.0×10^7	40.7	24.2	64.9	1.9	2.9×10^5	31.7	24.5	56.2	5.9
	NP_Phe	1.8×10^7	42.1	29.0	71.1	1.9	6.2×10^5	33.6	23.2	56.8	9.6

that the first two CytC molecules bind to the NP in the two topologically distinct 'polar' regions.

Binding Thermodynamics of NP−Protein Interactions. A global examination on the thermodynamic quantities listed in Table 1 reveals that the complexation of ChT with all particles features a favorable enthalpy change ($\Delta H < 0$), which is offset partially by unfavorable entropy loss ($\Delta S < 0$), affording overall free energy changes (ΔG) ranging from −32.2 to −34.4 kJ mol^{-1}. By contrast, the complexation of NPs with histone and CytC is endothermic, providing an unfavorable enthalpic contribution ($\Delta H > 0$) to the free energy of association. The binding of histone and CytC is, as a result, dominated by a large favorable entropy change ($\Delta S > 0$). The complexation behavior of proteins is a complex process that involves not only the synergetic work of noncovalent forces including electrostatic, hydrophobic, hydrogen bonding, and $\pi-\pi$ stacking but also features the desolvation of both NPs and proteins and solvation of newly formed complexes. The complexation process may be described in a simplified fashion using eq 1.

$$\text{protein}\cdot m\text{H}_2\text{O} + \text{NP}\cdot p\text{H}_2\text{O} \leftrightarrow [\text{protein}\cdot\text{NP}]\cdot(m + p - x)\text{H}_2\text{O} + x\text{H}_2\text{O} \quad (1)$$

According to eq 1, the thermodynamics of complexation depend on two simultaneous processes featuring noncovalent bond formation and solvent reorganization. From an enthalpic viewpoint, the formation of noncovalent bonds is exothermic ($\Delta H_{\text{intrinsic}} < 0$) while the disruption of structurally well-defined solvent shells is endothermic ($\Delta H_{\text{desolv}} > 0$). In this context, the intrinsic bond formation (or namely protein−particle interaction) plays a predominant role in the complex formation of ChT with NPs according to the observed negative enthalpy changes. It has been proposed that during protein−ligand interactions, solvent reorganization accounts for great contributions to enthalpy changes.[25] Nevertheless, the complex formation generally reduces the solvent-accessible surface area, resulting in the release of highly ordered solvent molecules into bulk solution. Consequently, the observed enthalpy changes are the compensatory outcomes of unfavorable desovlation enthalpy and favorable intrinsic enthalpy.[26]

Water molecules at interfaces can sometimes enhance the complementarity of the interacting surfaces;[27] however, the negative entropy changes do not necessarily indicate that the hydration of the complex interface remains unchanged or increases in comparison with that of the free proteins or protens and particles. Another important unfavorable contribution to the entropy change may arise from the conformational restriction of the flexible amino acid residues in both partners upon complexation. When the entropy increase due to desolvation is not large enough to remedy the entropy loss due to solute freedom reduction, overall unfavorable entropy changes are observed for the complexation of NPs with ChT.

In the complexation of NPs with histone and CytC, the large positive entropy change unambiguously indicates the disordering of molecules upon complex formation, presumably arising from the release of a large amount of the water of hydration from the binding interface. In comparison with ChT, histone and CytC possess more charged residues. Consequently, the corresponding interaction interfaces involve significantly more polar surface. The large entropic increase for the NP−histone and NP−CytC interactions may arise from either the release of more water of hydration or the dissociation of water molecules from a more ordered initial state.[28] Meanwhile, the breakage of well-defined solvent−protein and/or solvent−NP bonds leads to the unfavorable enthalpy changes, which counteract a portion of entropy contribution to the complex stability.

Hydrophobic Effects in NP−Protein Complexation. Complex stability between particles and ChT increases in the order of **NP_Glu** < **NP_Leu** < **NP_Phe** while with histone affinity increases in the order of **NP_Gly** < **NP_Ala** < **NP_Met**. These trends track well with the hydrophobicity of the particle surfaces. As we know that ChT has hydrophobic patches on the protein surface, these observations indicate the role of hydrophobic interactions in complex formation. To probe the hydrophobic effect, we investigated particle−ChT interactions at varying ionic strengths, since the electrostatic forces should be attenuated by the presence of competitive ions.[29] ITC experiments at various salt concentrations were carried out to quantify the corresponding thermodynamic parameters. The thermodynamic

(25) (a) Chervenak, M. C.; Toone, E. J. *J. Am. Chem. Soc.* **1994**, *116*, 10533−10539. (b) Swaminathan, C. P.; Surolia, N.; Surolia, A. *J. Am. Chem. Soc.* **1998**, *120*, 5153−5159. (c) Battistuzzi, G.; Borsari, M.; Ranieri, A.; Sola, M. *J. Biol. Inorg. Chem.* **2004**, *9*, 781−787.
(26) Shimokhina, N.; Bronowska, A.; Homan, S. W. *Angew. Chem., Int. Ed.* **2006**, *45*, 6374−6376.
(27) (a) Holdgate, G. A.; Tunnicliffe, A.; Ward, W. H. J.; Weston, S. A.; Rosenbrock, G.; Barth, P. T.; Taylor, I. W. F.; Pauptit, R. A.; Timms, D. *Biochemistry* **1997**, *36*, 9663−9673. (b) Li, Z.; Lazaridis, T. *J. Phys. Chem. B* **2005**, *109*, 662−670.
(28) (a) Makhatadze, G. I.; Privalov, P. L. *J. Mol. Biol.* **1993**, *232*, 639−659. (b) Privalov, P. L.; Makhatadze, G. I. *J. Mol. Biol.* **1993**, *232*, 660−679.
(29) Verma, A.; Simard, J. M.; Rotello, V. M. *Langmuir* **2004**, *20*, 4178−4181.

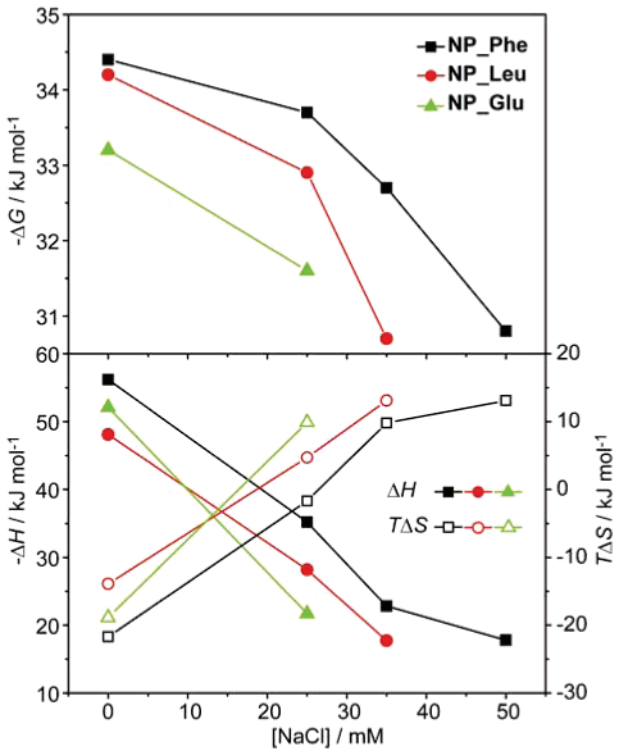

Figure 4. Thermodynamic parameters for the complexation of ChT with amino acid-functionalized NPs at various salt concentrations.

quantities for the complexation of ChT with three amino acid-functionalized NPs at various salt concentrations are presented in Figure 4 (see Table S1 for original data).

We can see from Figure 4 that the thermodynamic quantities depend critically on the monolayer components of NPs as well as the salt concentrations. As expected, the Gibbs free energy changes ($-\Delta G$) decrease with increasing salt concentration for all three NPs owing to the attenuation of electrostatic interactions. No binding was detectable for ChT−**NP_Glu** in 35 mM and ChT−**NP_Leu** in 50 mM or higher concentrations of NaCl solution, respectively. For **NP_Phe**, however, considerable complex stability is still preserved at 50 mM NaCl. In all cases, the binding constants increase in the order: **NP_Glu** < **NP_Leu** < **NP_Phe**. **NP_Phe** always affords higher binding affinity to ChT than **NP_Leu** does, although they have similar hydrophobicity indices. One plausible explanation is that the surface area of L-Phe is larger than that of L-Leu and can thus provide more efficient hydrophobic interactions with the protein. Additionally, there exists the possibility of CH−π interaction and $\pi-\pi$ stacking of L-Phe with residues in the ChT active pocket.[30]

At low salt concentrations, ChT−NP complexation is driven by enthalpy. With increasing salt concentration, the favorable enthalpic components decrease, whereas entropy changes become more favorable. In 50 mM of NaCl solution, the enthalpic and entropic contributions to the formation of ChT−**NP_Phe** complex are comparable. As hydrophobic interactions at room temperature are generally dominated by entropic effects,[31] the more positive entropic changes at higher salt concentrations presumably originate from hydrophobic interactions. Hydrophobic interactions, however, are not strong enough to maintain the complexes at higher ionic strength where electrostatic interaction is fully diminished.

Enthalpy−Entropy Compensation. It is apparent from Table 1 and Figure 4 that favorable enthalpy changes in protein−particle interactions are always balanced by entropic penalties and *vice versa*, i.e., enthalpy−entropy compensation. Although no explicit relationship between the enthalpic and the entropic terms can be deduced from fundamental thermodynamics, the compensation effect has been observed universally in host−guest complexation.[32] However, the origin of this extrathermodynamic relationship is still under controversy, complicated in part by experimental concerns regarding the quality of the data.[32b,33,34] In the current study, it should be noted that the use of ITC eliminates issues associated with van't Hoff approximations. Additionally, the wide range of free energy values provides an excellent benchmark for assessing compensation.[32b]

The physical significance of enthalpy−entropy compensation has been discussed in terms of cooperative interaction[35] and thermodynamic functions.[36] Inoue et al. have carried out quantitative correlation analyses of compensatory enthalpy−entropy relationships using a wide variety of molecular recognition systems.[37] In these analyses, the $T\Delta S$ value was linearly correlated with the ΔH value to give eq 2. When eq 2 is introduced to Gibbs−Helmholtz equation followed by the differential, eq 3 is obtained.

$$T\Delta S = \alpha\Delta H + T\Delta S_0 \quad (2)$$

$$\delta\Delta G = (1 - \alpha)\delta\Delta H \quad (3)$$

According to eq 3, the slope (α) of $\Delta H - T\Delta S$ plots reflects the contribution of enthalpic gains ($\delta\Delta H$) induced by alterations in host, guest, and/or solvent to the free energy change ($\delta\Delta G$), as some enthalpy has been canceled by the accompanying

(30) Shimohigashi, Y.; Nose, T.; Yamauchi, Y.; Maeda, I. *Biopolymers* **1999**, *51*, 9−17.
(31) Israelachvili, J. N. *Intermolecular and Surface Forces*, 2nd ed.; Academic Press: London, 1992.
(32) (a) Liu, L.; Guo, Q.-X. *Chem. Rev.* **2001**, *101*, 673−695. (b) Houk, K. N.; Leach, A. G.; Kim, S. P.; Zhang, X. *Angew. Chem., Int. Ed.* **2003**, *42*, 4872−4897. (c) Winzor, D. J.; Jackson, C. M. *J. Mol. Recognit.* **2006**, *19*, 389−407.
(33) Linert, W.; Han, L.-F.; Likovits, I. *Chem. Phys.* **1989**, *139*, 441−455.
(34) Sharp, K. *Protein Sci.* **2001**, *10*, 661−667.
(35) Williams, D. H.; Stephens, E.; O'Brien, D. P.; Zhou, M. *Angew. Chem., Int. Ed.* **2004**, *43*, 6596−6616.
(36) Dunitz, J. D. *Chem. Biol.* **1995**, *2*, 709−712.
(37) (a) Inoue, Y.; Wada, T. In *Advances in Supramolecular Chemistry*; Gokel, G. W., Ed.; JAI Press: Greenwich, CT, 1997; Vol. 4, pp 55−96. (b) Rekharsky, M. V.; Inoue, Y. *Chem. Rev.* **1998**, *98*, 1875−1917.
(38) (a) Aoki, K.; Taguchi, H.; Shindo, Y.; Yoshida, M.; Ogasahara, K.; Yutani, K.; Tanaka, N. *J. Biol. Chem.* **1997**, *272*, 32158−32162. (b) Myszka, D. G.; Sweet, R. W.; Hensley, P.; Brigham-Burke, M.; Kwong, P. D.; Hendrickson, W. A.; Wyatt, R.; Sodroski, J.; Doyle, M. L. *Proc. Nat. Acad. Sci. U.S.A.* **2000**, *97*, 9026−9031. (c) Morar, A. S.; Pielak, G. J. *Biochemistry* **2002**, *41*, 547−551. (d) Jung, H.-I.; Cooper, A.; Perham, R. N. *Biochemistry* **2002**, *41*, 10446−10453. (e) Buddai, S. K.; Toulokhonova, L.; Bergum, P. W.; Vlasuk, G. P.; Krishnaswamy, S. *J. Biol. Chem.* **2002**, *277*, 26689−26698. (f) Lukasik, S. M.; Zhang, L.; Corpora, T.; Tomanicek, S.; Li, Y.; Kundu, M.; Hartman, K.; Liu, P. P.; Laue, T. M.; Biltonen, R. L.; Speck, N. A.; Bushweller, J. H. *Nature Struct. Mol. Biol.* **2002**, *9*, 674−679. (g) Flatman, R.; McLauchlan, W. R.; Juge, N.; Furniss, C.; Berrin, J.-G.; Hughes, R. K.; Manzanares, P.; Ladbury, J. E.; O'Brien, R.; Williamson, G. *Biochem. J.* **2002**, *365*, 773−781. (h) Gell, D.; Kong, Y.; Eaton, S. A.; Weiss, M. J.; Mackay, J. P. *J. Biol. Chem.* **2002**, *277*, 40602−40609.
(39) (a) Filfil, R.; Chalikian, T. V. *J. Mol. Biol.* **2003**, *326*, 1271−1288. (b) Yokota, A.; Tsumoto, K.; Shiroishi, M.; Kondo, H.; Kumagai, I. *J. Biol. Chem.* **2003**, *278*, 5410−5418. (c) Girard, M.; Turgeon, S. L.; Gauthier, S. F. *J. Agric. Food Chem.* **2003**, *51*, 4450−4455. (d) Nielsen, P. K.; Bonsager, B. C.; Berland, C. R.; Sigurskjold, B. W.; Svensson, B. *Biochemistry* **2003**, *42*, 1478−1487. (e) Baerga-Ortiz, A.; Bergqvist, S.; Mandell, J. G.; Komives, E. A. *Protein Sci.* **2004**, *13*, 166−176. (f) Zhou, Y.-L.; Liao, J.-M.; Du, F.; Liang, Y. *Thermochim. Acta* **2005**, *426*, 173−178. (g) Kouadio, J.-L. K.; Horn, J. R.; Pal, G.; Kossiakoff, A. A. *J. Biol. Chem.* **2005**, *280*, 25524−25532. (h) Keeble, A. H.; Kirkpatrick, N.; Shimizu, S.; Kleanthous, C. *Biochemistry* **2006**, *45*, 3243−3254.

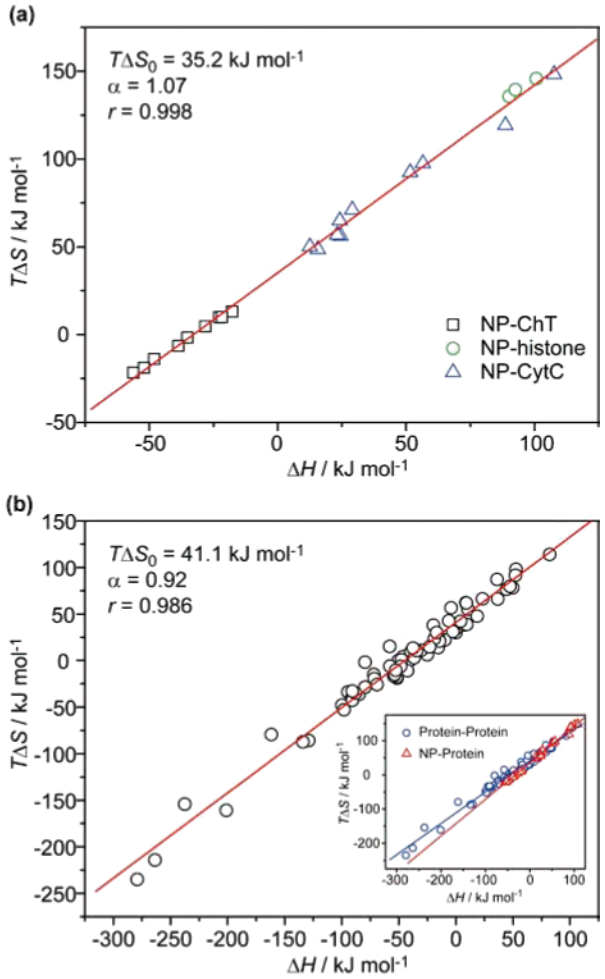

Figure 5. Plots of entropy ($T\Delta S$) versus enthalpy (ΔH) for (a) NP−protein (number of data set $n = 23$) and (b) protein−protein (number of data set $n = 70$) interactions.[15b,38,39] Thermodynamic quantities for protein−protein interactions are compiled in Table S2 in Supporting Information. Inset of part b shows the overlap of compensation plots for protein−protein and NP−protein interactions.

entropic loss ($\delta\Delta S$).[37] The intercept ($T\Delta S_0$) represents the inherent complex stability (ΔG) obtained at $\Delta H = 0$, which means that the complex is stabilized even in the absence of enthalpic stabilization in the case of positive $T\Delta S_0$ terms. By employing this correlation approach, the entropy changes ($T\Delta S$) listed in Table 1 and Figure 4 are plotted against corresponding enthalpy changes (ΔH) for the particle−protein systems studied. As shown in Figure 5a, an excellent linear relationship is obtained for these thermodynamic quantities with a correlation coefficient of 0.998. The compensation plot for protein−protein interactions is also depicted in Figure 5b for comparison (for original data see Table S2).

Using correlation analyses, it has been suggested that the slope (α) and the intercept ($T\Delta S_0$) can be empirically used as a quantitative measure of the conformational change and the desolvation upon complex formation, respectively.[37] In Table 2, the slope and intercept values of $\Delta H - T\Delta S$ plots for various host−guest complexation, protein−nonpeptide ligand (Table S3 and Figure S6), protein−peptide (Table S4 and Figure S7), and protein−protein interactions are compared with that of NP−protein interaction. As expected, rigid hosts such as cryptands and metal porphyrins give the smallest slope values, whereas flexible hosts such as glymes and lariat crown ethers show the

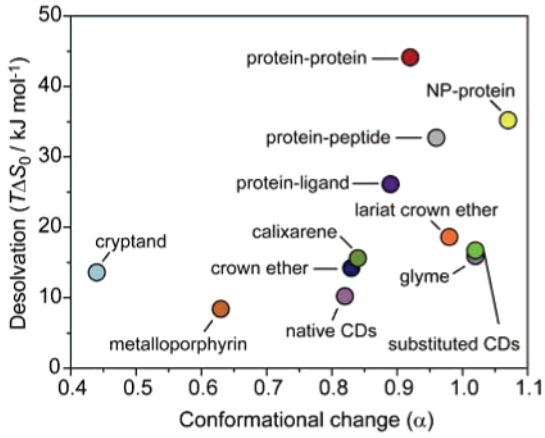

Figure 6. Slope (α) and intercept ($T\Delta S_0$) values for various host−guest systems. Protein−ligand interactions have been divided into protein−peptide and protein−other (protein−ligand) interactions.

largest slope values. The α value of particle−protein interaction is comparable to that of glyme−cation and substituted cyclodextrin−organic molecule interactions, and somewhat larger than that of protein−protein interaction (Figure 6). For the four systems involving protein partners, the α values increase in the order of nonpeptide ligand < protein < peptide < nanoparticle. This result indicates that the NP−protein couple undergoes large conformational changes during the complexation process. Such conclusion is in good accordance with the structural features of monolayer-protected NPs, as the flexible ligands are expected to reorganize on the NP surface to attain a maximum complex stability.[40]

While a number of host−guest systems feature slopes similar to protein−protein interactions, dramatic differences are observed in the intercept values ($T\Delta S_0$) of protein−partner interactions and other host−guest systems. For the protein−partner interactions, the intercept values ($T\Delta S_0$) increase in the order of nonpeptide ligand < peptide < nanoparticle < protein. The intercept for the particle−protein interactions is substantially more positive than that of the other 'small molecule' interactions and is comparable to protein−protein/peptide interactions. Protein surface recognition involves large surface contact area and the rearrangement of water of hydration around the binding interface. Therefore, the large intercepts explicitly indicate that the complexation of proteins with both native partners (i.e., proteins) and artificial receptors (i.e., NPs) experiences significant desolvation. As a consequence, the complex formation can be readily driven by the positive entropy changes due to the desolvation effect even in the absence of an enthalpic gain (i.e., $\Delta H = 0$). Obviously, for the protein−small ligand interactions, such a desolvation effect is not as significant as that of protein−protein and protein−particle interactions, as there is less desolvation process in this system although proteins also serve as a complexation partner.

Collectively, the enthalpy−entropy compensation analysis reveals large conformational changes and extensive desolvation during the formation of NP−protein complexes, consistent with the prototypical protein−protein interactions. Nanoparticles thus provide an excellent biomimetic system that affords both a large surface area and multivalent binding features.

(40) Boal, A. K.; Rotello, V. M. *J. Am. Chem. Soc.* **2000**, *122*, 734−735.

Table 2. Slope (α) and Intercept ($T\Delta S_0$) of Enthalpy−Entropy Compensation Plots for Various Host−Guest Systems

host	guest	α	$T\Delta S_0$/kJ mol^{-1}	data set (n)	r
glyme/podand[a]	metal ion	1.02	15.9	150	0.98
lariat crown ether[a]	metal ion	0.98	18.6	132	0.96
crown ether[a]	metal ion	0.83	14.2	744	0.92
cryptand[a]	metal ion	0.44	13.6	160	0.65
metal porphyrin[a]	pyridine/imidole	0.63	8.4	49	0.94
cyclophane/calixarene[a]	small organic molecule	0.84	15.6	77	0.92
native cyclodextrin[a]	small organic molecule	0.82	10.2	1091	0.90
substituted cyclodextrin[a]	small organic molecule	1.02	16.7	182	0.97
cyclodextrin[b]	small organic molecule	1.06	14.6		
organic host[b]	small organic molecule in water	0.96	13.2		
organic host[b]	small organic molecule in organic solvent	1.30	17.4		
protein	nonpeptide ligand	0.89	26.1	277	0.97
protein	peptide	0.96	32.7	252	0.98
protein	protein	0.92	44.1	70	0.99
nanoparticle	protein	1.07	35.2	23	0.99

[a] See ref 41. [b] Recalculated from reference 32b by assuming a temperature of 298.15 K, which presumably causes the deviation from the values obtained from ref 41.

Conclusion

In summary, we have demonstrated that electrostatic and hydrophobic interactions cooperatively control the complexation of amino acid-functionalized NPs with proteins, which depends on the surface distributions of charged and hydrophobic residues in the protein. ITC investigation revealed that the complexation of NPs with ChT is driven by enthalpy changes, while the complexation with histone and CytC is entropy-controlled. With ChT as a model protein, it is demonstrated that the electrostatic and hydrophobic contributions to the complex stability can be tuned by varying system ionic strengths. The validity of enthalpy−entropy compensation has been examined for the NP−protein system. An excellent linear relationship is obtained for the $\Delta H - T\Delta S$ plot with a near unit slope and a large intercept. These quantitative measurements indicate significant conformational changes and substantial dehydration of the partners, mimicking natural protein−protein interactions. These studies also point to strategies that can be used to further optimize synthetic receptors for proteins, namely the reduction of the slope (α) value while maintaining or enhancing the intercept ($T\Delta S_0$) value. Efforts to engineer particle surfaces to this end are currently underway.

Experimental Section

Materials. Amino acid-functionalized gold nanoparticles (NPs) were prepared by place-exchange of corresponding thiol ligands with 1-pentanethiol-capped gold NPs (diameter ∼ 2 nm) according to the published procedure.[17a,42] α-Chymotrypsin (Type II from bovine pancreas, ChT), cytochrome *c* (from equine heart), and histone (Type III-S from calf thymus, an isolated lysine rich fraction) were purchased from Sigma and used as received. Disodium hydrogen and sodium dihydrogen phosphate were dissolved in 18 MΩ water to make a 5 mM phosphate buffer solution of pH 7.4, which was used as solvent in isothermal titration calorimetries.

Isothermal Titration Calorimetry. An isothermal titration calorimeter (ITC) (Microcal Inc., Northampton, MA) was used in all microcalorimetric experiments operated at 30 °C. Each microcalorimetric titration experiment consisted of 30−45 successive injections of a constant volume (6 μL/injection) of ChT, CytC, or histone solution (150 μM to 400 μM according to binding ratio) into the reaction cell (1.4 mL) charged with a NP solution (1.0 to 2.5 μM) in the same buffer. The heat of dilution of the protein solutions when added to the buffer solution in the absence of NPs was determined in each run, using the same number of injections and concentration of proteins as in the titration experiments. The dilution enthalpies determined in these control experiments were subtracted from the enthalpies measured in the titration experiments. The ORIGIN program supplied by Microcal Inc. was used to calculate the binding constant (K_S) and molar enthalpy change (ΔH) of reaction from the titration curve. The molar Gibbs free energy changes (ΔG) and entropies (ΔS) of reaction were calculated from the experimentally determined K_S and ΔH values.

Acknowledgment. This research was supported by the National Institutes of Health (GM077173) and the NSF (NSEC, DMI-0531171, and MRSEC instrumentation).

Note Added after ASAP Publication: After this article was published on the Internet, the Supporting Information was replaced by a revised and correct version on August 6, 2007.

Supporting Information Available: Seven figures (Figures S1 to S7) and four tables (Tables S1 and S4) describing particle characterization, ITC plots, and literature values used in Figures 5 and 6 and Table 2. This material is available free of charge via the Internet at http://pubs.acs.org.

JA071642Q

(41) Liu, Y.; You, C.-C.; Zhang, H.-Y. *Supramolecular Chemistry: Molecular Recognition and Assembly of Synthetic Receptors*; Nankai University Press: Tianjin, 2001; pp 454−596 (in Chinese), ISBN 7-310-01641-6.

(42) TEM measurements on **NP_Ala** revealed an average particle size of 2.1 ± 0.4 nm (Figure S1). TGA revealed that the weight percentage of organic ligands in the NPs is 36% (Figure S2). Accordingly, the average molecular weight of the NP is estimated as 100 kDa, which was used for the preparation of NP solutions.